Proceedings World Geothermal Congress 2020+1
Reykjavik, Iceland, April - October 2021

An Advanced Well and Reservoir Model for Supercritical and Saline Geothermal Applications, the Example of IDDP-2

Benoit Lamy-Chappuis, Alina Yapparova and Thomas Driesner

Institute of Geochemistry and Petrology, ETH Zürich, Clausiusstrasse 25, CH-8092 Zürich, Switzerland

benoit.lamy-chappuis@erdw.etchz.ch

Keywords: Multi-segment well model, geothermal reservoir modelling, IDDP-2

ABSTRACT

The use of deep supercritical resources for geothermal energy production is desirable given the high energy density and low viscosity of supercritical fluids. However, the lack of practical experience and the usually poor characterization of such geothermal reservoirs makes predictions on the resource producibility and recharge particularly challenging.

Salty fluids add a layer of complexity due the varying phase relations ranging from Vapor (V) + Halite (H) near magmatic intrusions through V + Liquid (L) + H or V + L at shallower levels to possibly L and/or V near the surface. In the reservoir, these relations will be sensitive to cold meteoric water injection and well production. Well hydrodynamics will also be affected, especially if multiple interacting feed zones exist at different depths.

We upgraded to 3D an existing transport simulator (Weis, 2015) that was previously used for supercritical resource simulations (Scott et al., 2015). We coupled it to a newly developed multi-segment well model. Mass, energy and momentum conservation equations for the well are coupled and solved via an iterative Newton-Raphson procedure. The phases possibly present include L + V + H + Air. The thermodynamic properties in both the reservoir and the well are evaluated with the equation of state from Driesner and Heinrich (2007) which is valid in wide temperature (0-1000 °C), pressure (0-5000 bars) and salinity (0 to 100 wt%) range.

We conduct a comprehensive modelling for the IDDP-2 well in Reykjanes, a preliminary step is to reproduce the natural state of the surrounding system which necessitate the incorporation of sufficient geological constraints (permeability layering, presence of a magmatic intrusion, etc…). We let the system evolve for thousands of years from a range of hypothetical initial conditions until a good pressure and temperature match is found between the model and the field data.

Using the results from this preliminary study as a starting point, we assess the productivity potential of IDDP-2. We constrain the injectivity of the completions by replicating the results from a cold water injectivity test. Given the parameters of the well and formation and provided that the formation temperature as increased back to "pre" cold water injection levels, we find that the IDDP-2 well should self-flow. A possible explanation for IDDP-2 current startup issues is that after years of sustained cold water injection, the well and formation are still too cold.

1. INTRODUCTION

Wells drilled in the IDDP (Iceland Deep Drilling Project) framework pose new challenges to reservoir and well modelling as they can reach temperatures up to 500-600°C and could tap into highly saline formations. From the industrial point of view, once a geothermal resource has been identified, usual key questions are: what is the producibility and recharge of this resource? Embedded into the producibility question is the question of how to start the well. A proper answer to this requires an accurate representation of the well and reservoir dynamics prior to and during the startup attempt.

Here we focus on the IDDP-2 well, our goal being to better characterize possible well behavior in the context of a realistic model of the reservoir, including fluid state and properties at depth, and simulate its startup. In order to reach this goal, we model the formation of the geothermal system in response to a magmatic intrusion for several thousands of years aiming at reproducing the current state of the system. The well modelling is then performed within this natural state of the system, not including any production history of the geothermal operation at Reykjanes.

We develop a multi segment well model able to handle accurately the thermodynamics of the H_2O-NaCl system to magmatic temperatures as the currently best proxy for the saline Reykjanes system. Another important feature of this new model is the inclusion of a moving water table that is treated as a moving pressure boundary condition and where the mass and energy are discontinuous.

2. FIELD SCALE SIMULATION OF THE REYKJANES GEOTHERMAL SYSTEM NEAR IDDP-2

A preliminary step to simulating IDDP-2 well operations is to reproduce the current state of the surrounding formation. The parameters that we aim to reproduce are the current fluid pressures and temperatures along the well. The main focus is the temperature since it will control the density and therefore pressure.

Factors controlling the temperature distribution are principally heat sources and permeability structure. We test different scenarios by varying the permeability structure, simulating energy and mass transport for up to 10000 years. The field scale transport simulations are conducted using a control volume finite element scheme developed on the CSMP++ platform (Weis, 2015).

The model is 12x12x8.5 km large, with the top boundary located at 500 m depth, where the water table is thought to be located. The top boundary condition at initialization is 50°C and 1 bar. The IDDP-2 well is centered in this volume and extend vertically down to 4500 m depth.

A key feature of all the field scale simulations is the presence of a dry magmatic intrusion. Using the thermal anomaly results from Hokstad et al. (2017) we place the magmatic intrusion just below the well, starting at 5 km depth and extending by 3 km in the vertical direction and 1.5 km in both horizontal directions. At the start of the simulation this volume is at 950°C. Additionally, we prescribe a 200 mW/m^2 basal heat flux. The deciding factor to successfully reproduce the temperature distribution is the permeability structure. We define three (isotropic) permeability zones.

Since the uppermost kilometer displays a conductive temperature gradient of about 250°C/km, we associate a low permeability (1e-16 m^2) to this region. This likely corresponds to a hydrothermally altered caprock which presence is also attested by a steam cap visible in the gravitational anomaly data from Hokstad et al. (2017).

Below the caprock lies a 2.2 km thick layer where the temperature gradient sharply falls to 15°C/km with an average temperature of 280°C. This indicates strong fluid convection in this interval. By successive refinements, trying to match both the average temperature and temperature gradient we established that the permeability for this region should be 7e-15 m^2.

The top of the IDDP-2 slotted liner happens to be located just below this high permeability region, at about 3.2 km depth. It then extends to 4.5 km depth, going through a low permeability region. In this third region, the temperature gradient is again conductive (150°C/km) and the modelled permeability for this region decays from 1e-16 and 1e-22 m^2 in the 500 to 600°C temperature window. This corresponds to the brittle ductile transition whereby the permeability shut off as the rock becomes more malleable. The start of the brittle ductile transition at 500°C is supported by drilling observations, the rock becoming rubbery at this temperature. Due to the presence of the magmatic intrusion just beneath it, the brittle ductile transition occurs close to bottom of the well (4.5 km).

In the model, apart from the permeability heterogeneity, the host rock is otherwise homogeneous, with: 5% porosity, 800J/K heat capacity, 2W/(m.K) thermal conductivity, 2500 kg/m^3 density and 1e-10 Pa^{-1} compressibility.

Overall, using these parameters, a good match is found between field and simulation data. The results are summarized in Figure 1.

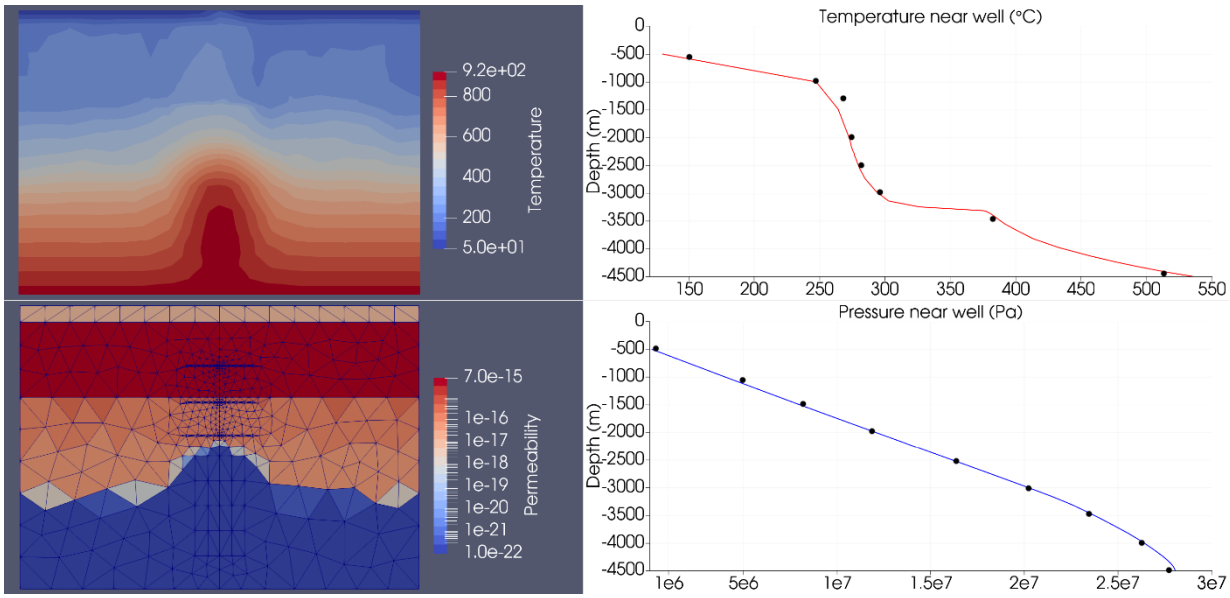

Figure 1: Left: temperature and permeability cross-sections of the Rekjanes model. The hot temperature anomaly is caused by the presence of a magmatic intrusion. On the bottom left, the mesh is represented, which shows mesh refinement around the well and completions. Right: pressure and temperature profiles at the well location, both simulated (curves) and data (black dots).

3. MULTI SEGMENT WELL MODEL

We develop a multi segment well model capable of handling thermodynamic properties encountered at IDDP-2. To this end, we use the EOS form Driesner and Heinrich (2007) that is valid in a wide range of pressure, temperature and NaCl content, namely: 0 to 5000 bars, 0 to 1000°C and 0 to 100% NaCl.

Conservation equations to be computed include: water mass conservation, salt mass conservation, momentum conservation and energy conservation. The primary variables associated with these equations are fluid mixture velocity, bulk salt mass fraction, fluid mixture pressure and bulk specific enthalpy.

Here, fluid mixture refers to assemblage of multiple fluid phases present in the well, liquid, vapor or supercritical, all possibly containing some amount of dissolved NaCl. We use a homogeneous flow model, i.e. all phases flow at the same velocity. Consequently, we neglect slippage between the phases that could affect their momentum. We also do not consider capillary effect and as a result all phase pressures are equal.

Bulk refers to the assemblage of a fluid and solid NaCl (halite). Halite is assumed to precipitate on the walls of the well and be immobile, it does not affect the density of the water column but can modify the cross-sectional area of the well. Salt mass and energy conservation are both evaluated for the bulk composition (fluid + halite). Given these assumptions, all phases share the same temperature.

Segments where fluid is absent should contain air. The air is assumed to have no mass or energy, therefore the only relevant equation for those segments is the one of pressure, which is then equal to the well head pressure. The well head pressure propagates down to the water table surface, located in a partially fluid saturated segment.

Given this formalism and assumptions we consider the following conservation equations, the mass conservation is written:

$$\frac{\partial \rho_f}{\partial t} = -\frac{\partial \rho_f \boldsymbol{u}}{\partial x} + Q_f \tag{1}$$

where ρ_f is the fluid mixture density, $\boldsymbol{u}$ the mixture velocity and the space increment ∂x is in the direction of the well segment. The fluid source Q_f can stem from water injection from the top of the well or exchange with the formation.

The momentum conservation with the homogenous flow model is written:

$$\frac{\partial P}{\partial x} = \rho_f \boldsymbol{g} cos(\theta) + \frac{f \rho_f \boldsymbol{u}|\boldsymbol{u}|}{4 r_w} + \frac{\partial \rho_f \boldsymbol{u}}{\partial t} + \frac{\partial \rho_f \boldsymbol{u}^2}{\partial x} \tag{2}$$

where $\boldsymbol{g}$ is the gravity acceleration, f is the Moody friction factor, r_w is the radius of the flowing section of the well and θ the well inclination. The Moddy friction factor is written:

$$f = \begin{cases} \frac{16}{Re} \\ \frac{1}{16}\left(log10\left(\frac{\xi}{3.7 r_{eff}} - \frac{5.02}{Re} log10\left(\frac{\xi}{3.7 r_{eff}} + \frac{13}{Re} \right) \right) \right)^{-2} \end{cases} \tag{3}$$

where ξ is the roughness of the pipe, r_{eff} is the radius of flowing cross section of the pipe (halite removed) and Re is the Reynolds number.

The bulk energy (fluid + halite) conservation is written:

$$\frac{\partial U}{\partial t} = -\frac{\partial \rho_f \boldsymbol{u}\left(h_f + \frac{1}{2}\boldsymbol{u}^2\right)}{\partial x} + \rho_f \boldsymbol{u} \boldsymbol{g} cos(\theta) - Q_{loss} + Q_h \tag{4}$$

where U contains the internal and kinetic energy of the fluid and halite phases. The transport of energy is only carried out by the fluid. The term Q_{loss} is the conductive heat exchange between the well and the formation. The heat loss model currently implemented uses the Ramey transient heat loss function (Ramey, 1962):

$$Q_{loss} = \frac{2\pi k (T_{well} - T_\infty)}{-\ln\left(\frac{r_w}{2\sqrt{\alpha t}}\right) - 0.29} \tag{5}$$

where k is the formation thermal conductivity, T_{well} is a well segment temperature, T_∞ is the ambient formation temperature near the segment, r_w is the well radius and α is the formation thermal dispersivity. Here we neglected the temperature gradient between the outside casing and the center of the well.

Finally, the salt mass conservation equation:

$$\frac{\partial C_{NaCl}}{\partial t} = -\frac{\partial \rho_f \boldsymbol{u} X_f}{\partial x} + Q_{NaCl} \tag{6}$$

where C_{NaCl} add the contributions of the fluid and halite while salt transport is only carried out by the fluid. X_f is the salt mass fraction of the fluid mixture.

The source terms Q_f, Q_h , Q_{NaCl} are calculated using an inflow performance relationship based on the Peaceman formula (Peaceman, 1977), for instance for the mass source:

$$Q_f = W \lambda_{tot} P_d \left(\rho_f m_l + \rho_f m_v \right) \tag{7}$$

where λ_{tot} is the total relative mobility of the reservoir fluid, with the contribution from the liquid phase being null if the liquid saturation is inferior to 0.3. P_d is the pressure drawdown and m is the mass fraction of a given phase. The term $\rho_f m_l + \rho_f m_v$ is upwinded. The first term $= 2\pi L_c \frac{K}{\ln\left(\frac{r_e}{r_w} + S\right)}$, is the well index, where L_c is the completion length, K, the formation permeability, S the skin factor and r_e the equivalent radius. The equivalent radius is $\sqrt{\frac{V/L_c}{\pi}}$, where V is the reservoir control volume associated with the well completion.

The partial differential equations are discretized using a time implicit and 1D upwind finite difference discretization. Below are the discretized momentum, mass, energy and salt mass conservation equations written in residual form:

$$R_M = P_N - P_{N-1} - \left[\rho_f \mathbf{g}\cos(\theta)\, L(1-S_{air})\right]_{N-1} + \left[\frac{f\rho_f \boldsymbol{u}|\boldsymbol{u}|}{4r_w} L(1-S_{air})\right]_{N-1} + \left[\frac{L}{dt}\left((1-S_{air})\rho_f \boldsymbol{u} - (1-S_{air})\rho_f \boldsymbol{u}\right|^{K-1}\right)\Big]_{N-1} + \left[(1-S_{air})\rho_f \boldsymbol{u^2}\right]_N - \left[(1-S_{air})\rho_f \boldsymbol{u^2}\right]_{N-1} \tag{8}$$

$$R_C = L_N\left[\rho_f(1-S_{air})A_{eff} - \rho_f(1-S_{air})A_{eff}\right|^{K-1}\Big]_N - \left[\rho_f A_{eff}\right]_{N-1}\boldsymbol{u}_N dt_{in} + \left[\rho_f A_{eff}\right]_N \boldsymbol{u}_{N+1} dt_{out} - q_f \tag{9}$$

$$R_U = L_N\left[(1-S_{air})A_{eff}(\rho_f h_f - P) - (1-S_{air})A_{eff}(\rho_f h_f - P)\right|^{K-1}\Big]_N + L_N[AS_h\rho_h h_h - AS_h\rho_h h_h)|^{K-1}]_N + L_N\left[(1-S_{air})A_{eff}(\rho_f \tfrac{\boldsymbol{u^2}}{2}) - (1-S_{air})A_{eff}(\rho_f \tfrac{\boldsymbol{u^2}}{2})\right|^{K-1}\Big]_N - \left[\rho_f h_f A_{eff}\right]_{N-1}\boldsymbol{u}_N dt_{in} + \left[\rho_f h_f A_{eff}\right]_N \boldsymbol{u}_{N+1} dt_{out} - \left[\rho_f \tfrac{\boldsymbol{u^2}}{2} A_{eff}\right]_{N-1}\boldsymbol{u}_N dt_{in} + \left[\rho_f \tfrac{\boldsymbol{u^2}}{2} A_{eff}\right]_N \boldsymbol{u}_{N+1} dt_{out} - A_{eff} L\rho_f(1-S_{air})\boldsymbol{u}\boldsymbol{g}cos(\theta) dt_{in} - q_{loss} - q_h \tag{10}$$

$$R_S = L_N\left[\rho_f X_f(1-S_{air})A_{eff} - \rho_f X_f(1-S_{air})A_{eff}\right|^{K-1}\Big]_N + L_N[AS_h\rho_h - AS_h\rho_h|^{K-1})]_N - \left[\rho_f X_f A_{eff}\right]_{N-1}\boldsymbol{u}_N dt_{in} + \left[\rho_f X_f A_{eff}\right]_N \boldsymbol{u}_{N+1} dt_{out} - q_{NaCl} \tag{11}$$

where N is the segment index and K the time level.

The advection terms in the mass, energy and salt mass residuals are written for the upflow case, four configurations can exist for any given segment: upflow, downflow, convergent flow (coming in from both ends) and divergent flow (going out on both ends). All conservation equations have been scaled by the air saturation S_{air} which is the proportion of air in the volume LA_{eff}, where L is the length of the segment and $A_{eff} = A(1-S_h)$ is the effective cross area of the segment, once halite is removed. Similarly, the terms dt_{in} and dt_{out} have been introduced, which can be a fraction of dt or even null in segments where the water table is located. For example, for upflow in a partially air saturated segment $dt_{out} = 0$ and dt_{in} is the time since the water table reached this segment.

The coupled system of equations is then solved iteratively using the Newton-Raphson method. The well-formation pressure coupling is also solved iteratively in a partially implicit manner. A graph of the global solution method is shown in Figure 2.

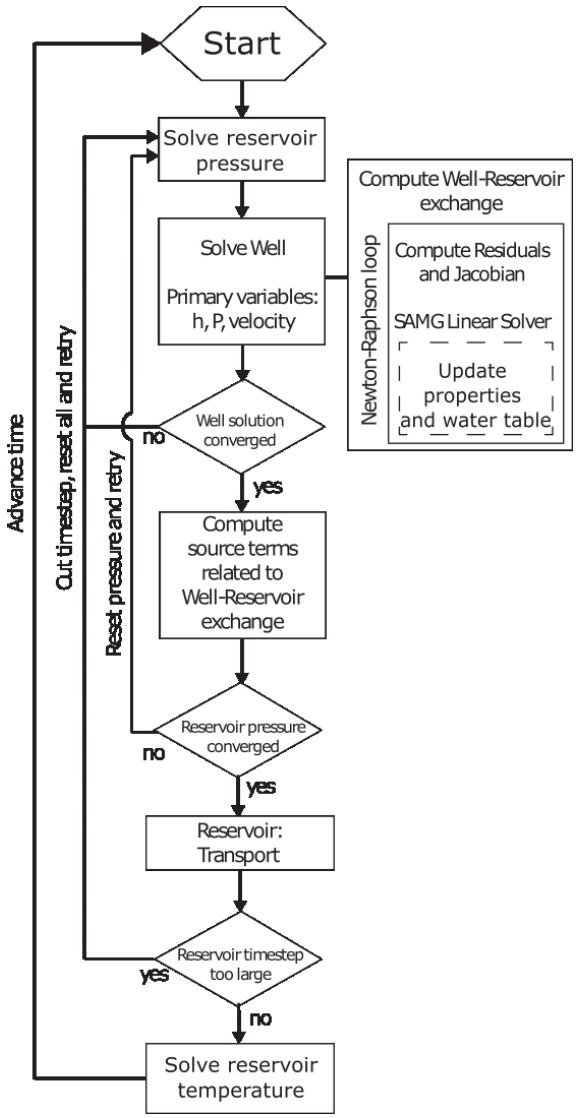

Figure 2: Solution method for the well and reservoir.

4. IDDP-2 FLOW SIMULATIONS

The modeled well extend vertically from the surface to a depth of 4500 m. The radius of the flowing cross section is 11 cm in the 1300 to 2900 m interval and 8 cm otherwise. The whole well has a constant roughness of 0.5 mm. The well is divided in 45 segments with lengths varying from 30 m near the completions to 150 m.

To evaluate the permeability of the completions we simulate the cold water injectivity test carried out in January 2017, see Sæther (2020), we inject 10°C fresh water at a rate of 42.5 l/s. Based on the test results we assume that there are three main completions. Two completions located in the third (low permeability) region where the well likely intercept thin fracture zones at 3.4 and 4.4 km. These fracture zones are explicitly represented in the 3D mesh as 30 m thin horizontal layers, 1 km in radius, centered around the well. The third well completion is located in the convective layer at 2.3 km and is due to casing damage, we assume that this completion is 10 m long.

We then adjust the permeability of the completions in order to replicate the measured temperature and pressure profiles. The best match was found for the following completion permeabilities: 7e-15 m^2 at 2.3 km, 4e-14 m^2 at 3.4 km and 4e-16 m^2 at 4.4 km, the results are shown in Figure 3. The permeability at 3.4 km needs to be 100 times the permeability at 4.4 km to explain the bend in the temperature profile at 3.4 km. The absolute permeability values have then been adjusted to match the pressure profile and the water table depth (about 800 m). The permeability at 2.3 km correspond to the formation permeability used in the prior field scale modelling. Most of the injected water is exiting at 3.4 km where the completion permeability is very large.

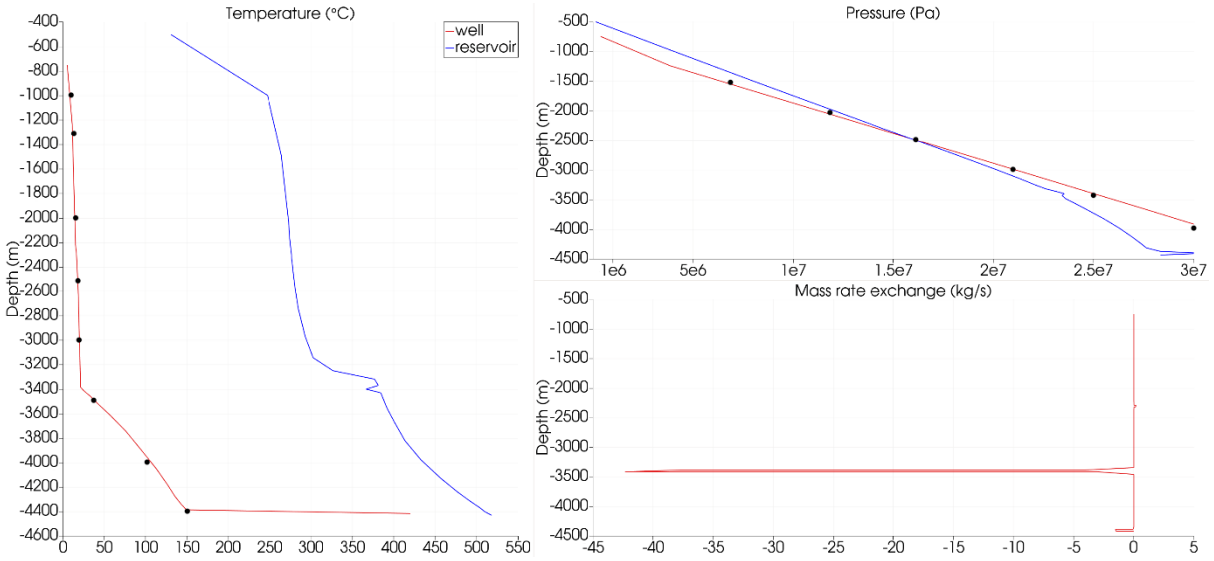

Figure 3: Simulated cold water injectivity test, after 10 hours of injection. Simulated pressure and temperature profiles in blue for the reservoir and red for the well, black dots are field data. A negative mass exchange means outflow from the well. After 10 hours of injection a small cooling effect can be seen in the formation at 3400 m.

Starting from the results shown in Figure 3, we stop injection after 10 hours and wait for the well and surroundings to warm up, as the well fluid warms up, it remains less dense than the formation fluid due to its lower salinity. This leads to inflow at 3.4 and 4.4 km and outflow at the damage zone. After two days, the configuration of the well is then as shown in Figure 4.

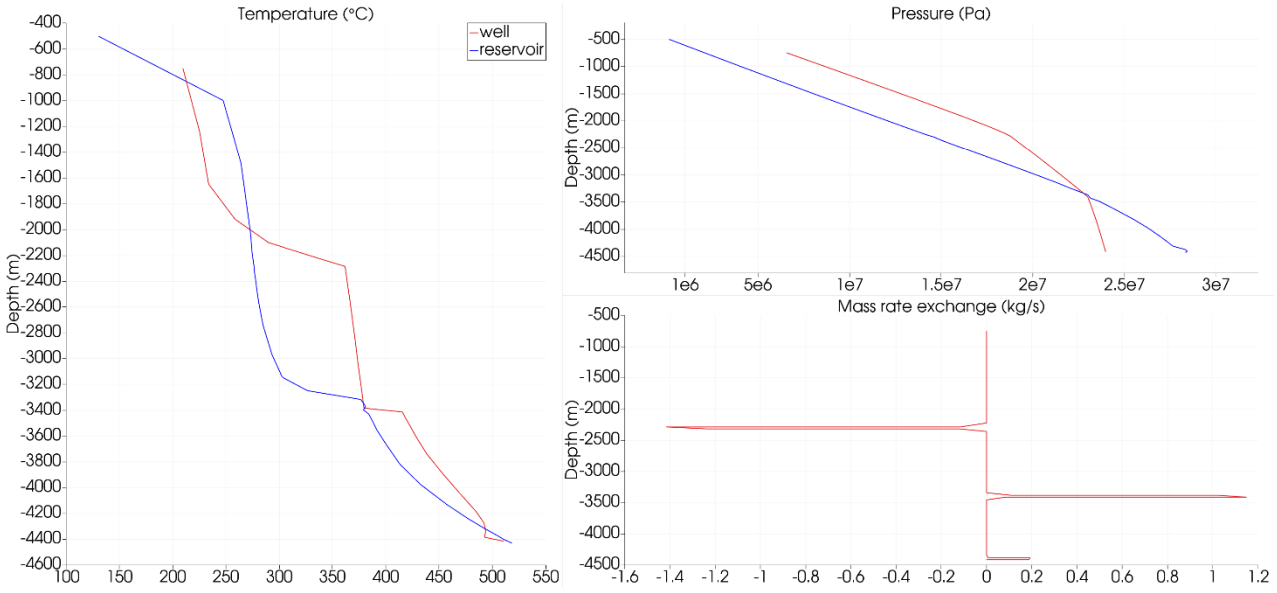

Figure 4: Well state 2 days after the end of the cold water injection. The warming up of the well and formation is fast because the cold water injection phase was only simulated for 10 hours.

Fluid upflow and warming up are restricted in the top 2 km of the well due to the leak at the damage zone. Nevertheless, this upflow together with heat conduction is sufficient to completely warm up the well and raise the water table to the surface after one more day. Provided that the formation is warm, no particular startup procedure seems necessary to start up the well. With continued warming, the wellhead pressure needs to be raised in order to avoid complete boiling of the well. As the water table reaches the surface, the well state is as shown in Figure 5.

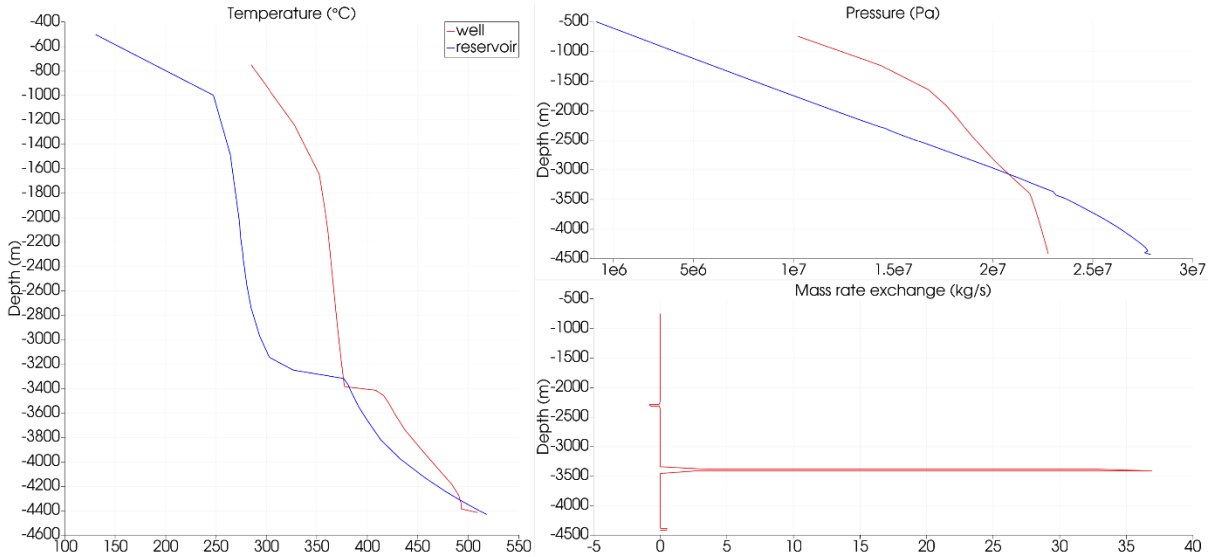

Figure 5: Self-flowing IDDP-2 well configuration at breakthrough.

The output at the wellhead is about 35 kg/s at a temperature of 250°C. Due to its high permeability, most of the well production originates from the completion at 3.4 km. The incidence of the casing damage at 2.3 km is very limited, with a 1 kg/s leak.

5. CONCLUSION

Using a new multi-segment well model we are able to simulate deep geothermal wells such as IDDP-2. Our workflow consists in modelling the system at the field scale first in order to better capture the natural state of the formation. Well operations simulation, such as cold water injection or air pressurization can then be carried.

We use existing in-situ measurements to better characterize the well and in particular, to evaluate the permeability of the completions. We find that it is possible to enable IDDP-2 to self-flow without using an air compression startup procedure. This is assuming that the well and formation have sufficiently warmed up and that there is no blockage. However, given the presence of a dominant completion at 3.4 km depth, it is not possible to produce fluids from deeper and therefore more desirable parts of the well.

There remains uncertainty about the current flowing conditions at IDDP-2 and it seems necessary to further validate our model with current in-situ data. In particular we need to model the full cold water injection period which already lasted several years at a reduced rate. Currently, the IDDP-2 well is open to atmospheric pressure and is not self-flowing, the water table is sitting at about 700 m. This is likely due to the well and formation still being too cold. In future work we will try to confirm that the well and formation are indeed too cold to allow the well to self-flow and if that is the case we will evaluate the possibility of using air compression as a mean to start the well in this cold configuration.

ACKNOWLEDGMENTS

We would like to thank Equinor for funding this research. We thank Sturla Sæther, Jostein Alvestad and Kent Holing from Equinor for providing guidance and helpful suggestions during this project.

REFERENCES

Driesner, T., Heinrich, C.A., 2007. The system H2O-NaCl. Part I: Correlation formulae for phase relations in temperature-pressure-composition space from 0 to 1000 degrees C, 0 to 5000 bar, and 0 to 1XNaCl. Geochim. Cosmochim. Acta71 (20), 4880–4901.

Hokstad, K., Tänavsuu-Milkeviciene, K., 2017. Temperature Prediction by Multigeophysical Inversion: application to the IDDP-2 Well at Reykjanes, Iceland. GRC Transactions 41, 1141-1152.

Peaceman, D.W., 1977. Interpretation of well-block pressures in numerical reservoir simulation, SPE 6893, 52nd Annual Fall Technical Conference and Exhibition, Denver.

Ramey Jr., H.J., 1962. Wellbore heat transmission. J.Petrol.Technol. 225, 427–435.

Sæther, S., 2020. Estimating Flow Performance of IDDP-2/DEEPEGS Well by Introducing Local Injectivity Indexes for Different Reservoir Depths. Proceedings World Geothermal Congress 2020.

Scott, S., Driesner, T., and Weis, P., 2015. Geologic controls on supercritical geothermal resources above magmatic intrusions. Nature Communications 6, (2015), 7837.

Weis, P., 2015. The dynamic interplay between saline fluid flow and rock permeability in magmatic-hydrothermal systems. Geofluids15, 350–371.